

A study on density functional theory of the effect of pressure on the formation and migration enthalpies of intrinsic point defects in growing single crystal Si

Cite as: J. Appl. Phys. **111**, 093529 (2012); <https://doi.org/10.1063/1.4712632>

Submitted: 14 January 2012 • Accepted: 11 April 2012 • Published Online: 10 May 2012

Koji Sueoka, Eiji Kamiyama and Hiroaki Kariyazaki



View Online



Export Citation

ARTICLES YOU MAY BE INTERESTED IN

Density functional theory study on the impact of heavy doping on Si intrinsic point defect properties and implications for single crystal growth from a melt

Journal of Applied Physics **114**, 153510 (2013); <https://doi.org/10.1063/1.4825222>

A climbing image nudged elastic band method for finding saddle points and minimum energy paths

The Journal of Chemical Physics **113**, 9901 (2000); <https://doi.org/10.1063/1.1329672>

Intrinsic point defect incorporation in silicon single crystals grown from a melt, revisited

Journal of Applied Physics **110**, 063519 (2011); <https://doi.org/10.1063/1.3641635>

Journal of
Applied Physics

Special Topics Open for Submissions

Learn More



A study on density functional theory of the effect of pressure on the formation and migration enthalpies of intrinsic point defects in growing single crystal Si

Koji Sueoka, Eiji Kamiyama, and Hiroaki Kariyazaki

Department of Communication Engineering, Okayama Prefectural University, 111 Kuboki, Soja, Okayama 719-1197, Japan

(Received 14 January 2012; accepted 11 April 2012; published online 10 May 2012)

In 1982, Voronkov presented a model describing point defect behavior during the growth of single crystal Si from a melt and derived an expression to predict if the crystal was vacancy- or self-interstitial-rich. Recently, Vanhellefont claimed that one should take into account the impact of compressive stress introduced by the thermal gradient at the melt/solid interface by considering the hydrostatic pressure dependence of the formation enthalpy of the intrinsic point defects. To evaluate the impact of thermal stress more correctly, the pressure dependence of both the formation enthalpy (H_f) and the migration enthalpy (H_m) of the intrinsic point defects should be taken into account. Furthermore, growing single crystal Si is not under hydrostatic pressure but almost free of external pressure (generally in Ar gas under reduced pressure). In the present paper, the dependence of H_f and H_m on the pressure P , or in other words, the pressure dependence of the formation energy (E_f) and the relaxation volume (v_f), is quantified by density functional theory calculations. Although a large number of *ab initio* calculations of the properties of intrinsic point defects have been published during the last years, calculations for Si crystals under pressure are rather scarce. For vacancies V , the reported pressure dependences of H_f^V are inconsistent. In the present study, by using 216-atom supercells with a sufficient cut-off energy and mesh of k-points, the neutral I and V are found to have nearly constant formation energies E_f^I and E_f^V for pressures up to 1 GPa. For the relaxation volume, v_f^I is almost constant while v_f^V decreases linearly with increasing pressure P . In case of the hydrostatic pressure P_h , the calculated formation enthalpy H_f^I and migration enthalpy H_m^I at the [110] dumbbell site are given by $H_f^I = 3.425 - 0.057 \times P_h$ (eV) and $H_m^I = 0.981 - 0.039 \times P_h$ (eV), respectively, with P_h given in GPa. The calculated H_f^V and H_m^V dependencies on P_h given by $H_f^V = 3.543 - 0.021 \times P_h^2 - 0.019 \times P_h$ (eV) and $H_m^V = 0.249 + 0.018 \times P_h^2 - 0.037 \times P_h$ (eV), respectively. These results indicate that, when assuming that the pre-factors in the Arrhenius equation are not influenced, hydrostatic pressure up to 1 GPa leads to a slight increase of the thermal equilibrium concentration and diffusion of vacancies but this increase is much smaller than that of self-interstitials. The thermal stress in growing Si crystal is compressive, and thus the point defects are under internal pressure. Taking into account the differences in the enthalpies of point defects between hydrostatic pressure and internal pressure, Si crystal shifts to being V -rich with an increase in thermal stress during crystal growth. © 2012 American Institute of Physics. [<http://dx.doi.org/10.1063/1.4712632>]

I. INTRODUCTION

In 1982, Voronkov¹ presented a model describing point defect behavior during the growth of single crystal Si from a melt and derived a criterion to predict if the crystal was vacancy- or self-interstitial-rich. According to the Voronkov criterion, a crystal that is pulled with the ratio $\Gamma 0$ of pulling speed v over temperature gradient $G 0$ at the melt/solid interface, larger than a critical value $\Gamma 0_{crit}$, is vacancy-rich while when $\Gamma 0$ is smaller than the critical value, the pulled crystal is interstitial-rich. Published values for $\Gamma 0_{crit}$ range between 1.3 and $2.2 \times 10^{-3} \text{ cm}^2 \text{ min}^{-1} \text{ K}^{-1}$ and depend on the simulator that is used to calculate the thermal gradient and also on the doping and resistivity of the crystal.²⁻⁷

Abe and Takahashi⁸ proposed an alternative model whereby the growth interface is filled with vacancies only, and self-interstitials are generated in the growing Si crystal by thermal stresses. Recently, Vanhellefont claimed that

one should take into account the impact of stress introduced by the thermal gradient on $\Gamma 0_{crit}$ by considering the hydrostatic pressure dependence of the formation enthalpy of the intrinsic point defects.⁹ Stress control will be one of the major concerns in the development of future large diameter defect-free silicon crystals. To evaluate the impact of thermal stress more correctly, the pressure dependence of both the formation enthalpy and the migration enthalpy of the intrinsic point defects should be taken into account. Furthermore, growing single crystal Si is not under hydrostatic pressure but almost free of external pressure (generally in Ar gas under reduced pressure).

The purpose of this study is to quantify the dependence of H_f and H_m of the uncharged self-interstitial I and vacancy V on the pressure P , or in other words, the pressure dependence of the formation energy (E_f) and the relaxation volume (v_f), by density functional theory (DFT) calculations. Recently, a

large number of *ab initio* calculations of the properties of intrinsic point defects in Si crystals have been published.¹⁰ However, reports on calculations of the intrinsic point defect properties in Si crystals under pressure are rather scarce. For self-interstitials, to our knowledge, the only relaxation volumes calculated for *I* come from Centoni *et al.*,¹¹ besides an older calculation including the pressure dependence of E_f by Antonelli and Bernholc.¹² However, both the pressure dependence of E_f and v_f for *I*, i.e., the pressure dependencies of H_f and H_m were not reported. For vacancies, the reported pressure dependencies of H_f are inconsistent. Initially, Antonelli and Bernholc¹² obtained an increase of H_f of V under hydrostatic pressure while later Antonelli *et al.*¹³ and Centoni *et al.*¹¹ found a decrease, while Ganchenkova *et al.*¹⁴ concluded an increase of H_f under hydrostatic pressure. One of the goals of the present study is therefore also to try to clarify this contradiction for the vacancy.

The thermal stress in growing single crystal Si is compressive, and is not external but internal stress. Therefore, the point defects are under internal pressure. To estimate the impact of thermal stress on intrinsic point defects in growing Si, the differences in the formation volumes of point defects under hydrostatic pressure and under internal pressure should be considered.

Here, we consider the formation of a vacancy in perfect Si crystal (without any sinks or sources of vacancies) with finite sizes (surrounded by surfaces) under thermal equilibrium. To create V , one moves an atom from the interior to a surface site.¹⁵ This results in the volume increase of Ω_{Si} (= atomic volume) at the surface. Therefore, under hydrostatic pressure P_h , we need the work of $P_h(\Omega_{Si} + v_f^V)$ with the Ω_{Si} of the atomic volume and the v_f^V of the relaxation volume to form a vacancy. In Si crystal under thermal stress σ , on the other hand, we should not include the contribution of $P\Omega_{Si}$ as the surfaces are free of external normal stress.¹⁵ That is, under internal pressure P_{in} ($= \sigma$), we only need the work of $P_{in}v_f^V$ to form a vacancy. Taking this into account, we estimated the impact of thermal stress on Γ_{0crit} by using DFT results.

II. CALCULATION DETAILS

Density functional theory calculations were performed within the generalized gradient approximation (GGA) for

electron exchange and correlation, using the CASTEP code.¹⁶ The Kohn-Sham equation¹⁷ was solved self-consistently to obtain the ground state of the system for given atomic configurations. The wave functions were expanded with the plane waves, and the ultra-soft pseudo-potential method¹⁸ was used to reduce the number of plane waves. The cut-off energy was 340 eV. The expression proposed by Perdew *et al.*¹⁹ was used for the exchange-correlation energy in the GGA. The density mixing method²⁰ and Broyden - Fletcher - Goldfarb - Shanno (BFGS) geometry optimization method²¹ were used to optimize the electronic structure and atomic configurations, respectively. Periodic boundary conditions were used with cubic supercells of 216 atoms for calculations of perfect and defect-containing Si crystals. In simulations reported in the literature,^{22,23} the electronic properties and the volumetric relaxations of point defects, such as the Jahn-Teller distortion of a vacancy, are well reproduced using 216-atom supercells. k -point sampling was performed at $2 \times 2 \times 2$ special points in a Monkhorst-Pack grid,²⁴ which was sufficient to obtain converged results for 216 Si-atoms supercells.²⁵ The convergence condition of the electronic structure optimization was set at a total energy change smaller than 5×10^{-7} eV/atom. The convergence conditions of the geometry optimization were set at a total energy change smaller than 5×10^{-6} eV/atom, an atomic displacement smaller than 1×10^{-4} Å, an atomic force smaller than 0.001 eV/Å, and stress in the cell smaller than 0.001 GPa.

The reference point in this study was the perfect Si crystal. The total energies at different volumes were fit to a Birch-Murnaghan equation of state²⁶ as shown in Fig. 1(a). The equilibrium atomic volume Ω_{Si} in the present study was 20.39 Å³. The bulk modulus at $P = 0$ was $B_0 = 87.7$ GPa and its pressure derivative was $B'_0 = 4.02$. The pressure P in cubic cells with different volumes was determined by fitting to a Birch-Murnaghan equation of state with obtained Ω_{Si} , B_0 , and B'_0 . The pressures P in cubic cells with different volumes were also obtained analytically with the method by Nielsen and Martin.²⁷ The analytically obtained pressures P agreed well with those obtained by fitting to the Birch-Murnaghan equation of state as shown in Fig. 1(b). The estimated values of experimental thermal stress in growing Si crystal were several tens of MPa at the highest value.²⁸ Therefore, we did calculations up to 1 GPa with pressure P .

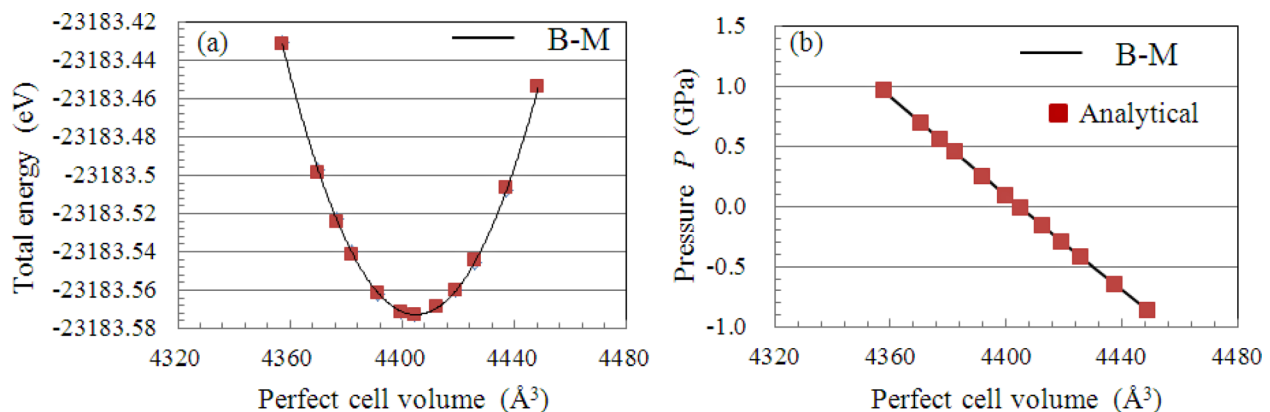


FIG. 1. (a) Calculated total energies of perfect cells at different volumes with fitting to a Birch-Murnaghan equation of state (B-M), and (b) comparison of analytically obtained pressures and those obtained by fitting to the Birch-Murnaghan equation of state (B-M).

Similar calculations were performed with cubic supercells containing point defects. In single crystal Si, the thermal equilibrium concentrations of self-interstitials I and vacancies V , even near melt temperature, are well below $5 \times 10^{15} \text{ cm}^{-3}$.⁹ For such low concentration, the calculation cells should be surrounded by perfect cells. These perfect Si crystals are assumed to deform isotropically under the pressure. Therefore, we also imposed a cubic shape for the defect-involving calculation cell. In each case, the supercells were set at a particular cubic volume and the ionic coordinates were fully relaxed to build up a list of energy-pressure-volume data points by using the analytically obtained P .

In the present study, only neutral point defects were considered. For the self-interstitial, the two lowest energy configurations, i.e., the [110] dumbbell (D) and the tetrahedral (T) sites were calculated. It is well known that, for neutral I , the [110] D-site is the lowest-energy configuration while the T-site is a transition state.^{10,11,23} A vacancy was introduced by eliminating one Si atom located around the center of each supercell. Further details on the point defect configurations considered in this study are given in Fig. 2 and will be commented on later.

The energy-pressure-volume data of perfect and defect-involving cubic cells were used to find the relationship between pressure P and (1) formation energy E_f and (2) relaxation volume v_f . The formation energies of I and V are obtained with,

$$E_f^I(P) = E_{\text{tot}}[\text{Si}_{216}\text{I}_1](P) - \frac{217}{216} E_{\text{tot}}[\text{Si}_{216}](P) \quad (1a)$$

and

$$E_f^V(P) = E_{\text{tot}}[\text{Si}_{216}\text{V}_1](P) - \frac{215}{216} E_{\text{tot}}[\text{Si}_{216}](P). \quad (1b)$$

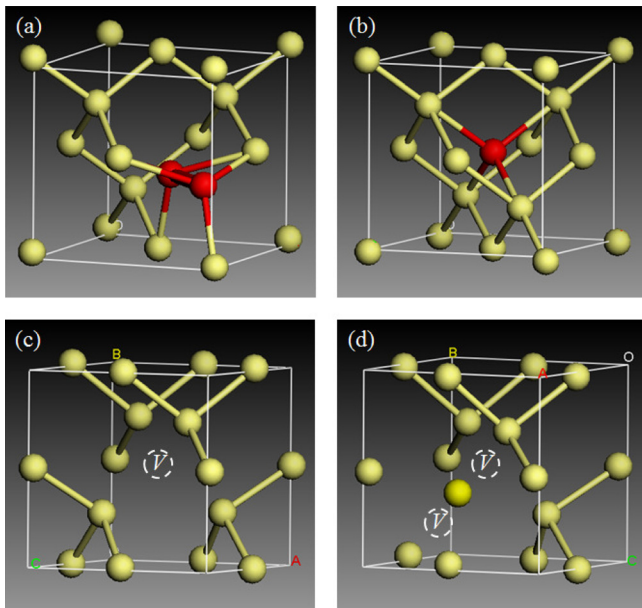


FIG. 2. Geometries of defects in relation to conventional cubic unit cell of Si. (a) D-site, (b) T-site, (c) h -JT, l -JT, T_d symmetry, and (d) split vacancy.

Here, $E_{\text{tot}}[\text{Si}_{216}\text{I}_1](P)$ and $E_{\text{tot}}[\text{Si}_{216}\text{V}_1](P)$ are the total energies of the cell including one I and V at pressure P , respectively. $E_{\text{tot}}[\text{Si}_{216}](P)$ is the total energy of the perfect cell at the same pressure P .

The relaxation volumes of I and V are obtained with,

$$v_f^I(P) = \text{Vol}[\text{Si}_{216}\text{I}_1](P) - \text{Vol}[\text{Si}_{216}](P) \quad (2a)$$

and

$$v_f^V(P) = \text{Vol}[\text{Si}_{216}\text{V}_1](P) - \text{Vol}[\text{Si}_{216}](P). \quad (2b)$$

Here, $\text{Vol}[\text{Si}_{216}\text{I}_1](P)$ and $\text{Vol}[\text{Si}_{216}\text{V}_1](P)$ are the volumes of the cell including one I and V at the pressure P , respectively. $\text{Vol}[\text{Si}_{216}](P)$ is the volume of the perfect cell at the same pressure P .

The formation enthalpies H_f of I and V under hydrostatic pressure P_h are obtained by using the formation volumes of I and V , i.e., $(-\Omega_{\text{Si}}(P_h) + v_f^I(P_h))$ and $(\Omega_{\text{Si}}(P_h) + v_f^V(P_h))$ with,

$$H_f^I(P_h) = E_f^I(P_h) + P_h \times (-\Omega_{\text{Si}}(P_h) + v_f^I(P_h)) \quad (3a)$$

and

$$H_f^V(P_h) = E_f^V(P_h) + P_h \times (\Omega_{\text{Si}}(P_h) + v_f^V(P_h)). \quad (3b)$$

Here, $\Omega_{\text{Si}}(P_h)$ is the equilibrium atomic volume at the hydrostatic pressure P_h .

Under internal pressure P_{in} in the growing Si crystal, the formation volumes of I and V are equal to the relaxation volumes of $v_f^I(P_{\text{in}})$ and $v_f^V(P_{\text{in}})$. The formation enthalpies of I and V under internal pressure P_{in} are obtained with

$$H_f^I(P_{\text{in}}) = E_f^I(P_{\text{in}}) + P_{\text{in}} \times v_f^I(P_{\text{in}}) \quad (4a)$$

and

$$H_f^V(P_{\text{in}}) = E_f^V(P_{\text{in}}) + P_{\text{in}} \times v_f^V(P_{\text{in}}). \quad (4b)$$

III. RESULTS AND DISCUSSION

A. Self-interstitials under hydrostatic pressure

As mentioned before, the T-site is a transition state for the neutral self-interstitial. Harrison²⁹ has proposed a set of corrections for DFT calculations and applied them to the neutral T -site in Si. The T interstitial ejects two electrons into the conduction band. Therefore, Harrison suggests a band gap correction for the too-small Local Density Approximation (LDA) band gap and an energy gain due to the formation of donor states for the two electrons. Due to the finite size of the cell, a part of the conduction band and the resonant p states in the conduction band are occupied, whereas in reality, the two electrons would reside in donor states below the bottom of the conduction band. In the present study, the gap-correction with two electrons in the conduction band leads to 1.016 eV at $P=0$. The calculated band gap within GGA decreases from 0.599 eV ($P=0$) to 0.581 eV ($P=1$ GPa). The decrease of the band gap, -0.018 eV, from $P=0$ to 1 GPa is

in very good agreement with the experimental value of -0.014 eV.³⁰ Therefore, we used 1.016 eV as constant value of gap-correction. For the finite-size correction, -0.348 eV was obtained, independent of pressure P . Band structures and density of states seem to indicate that the cells in the present study are large enough to allow for the formation of the donor states; therefore, we do not apply the respective (small) correction. Finally, we find $+0.668$ eV as the total correction of the formation energy of the T-site at zero pressure, which is close to the value estimated by Windl.²³

Figure 3 shows the calculated dependence of the formation energy E_f^I for the D-site and T-site on the pressure P up to 1 GPa. It was found that E_f^I is almost constant for pressures up to 1 GPa. The formation energies are 3.425 eV for the D-site and 4.406 eV for the T-site at $P=0$. That is, the migration energy of I at $P=0$ is 0.981 eV. The obtained formation energy for the neutral D-site is in good agreement with previous DFT studies with GGA yielding values between 3.2 eV and 3.7 eV.¹⁰ The obtained $H_f^I + H_m^I$ ($=4.406$ eV) at $P=0$ is also close to the older experimental value of 4.68 eV (Ref. 31) and the more recent value of 4.95 eV.^{32,33}

Figure 4 shows the calculated dependence of the relaxation volume v_f^I for the D-site and T-site on the pressure P up to 1 GPa. It was found that the relaxation volumes of I for the D-site and the T-site are also quasi independent of pressure. The relaxation volume, v_f^I , and the formation volume ($-\Omega_{Si} + v_f^I$) of D- and T-sites are summarized in Table I with the DFT results reported by Centoni *et al.*¹¹ at $P=0$.

Figure 5 shows the dependence of the formation enthalpy H_f^I for D-site and T-site on the hydrostatic pressure P_h obtained with Eq. (3a). It was found that the formation enthalpies of I decrease linearly with increasing hydrostatic pressure P_h . The calculations yield formation and migration enthalpies of the neutral I at the D-site that are given by

$$H_f^I = 3.425 - 0.057 \times P_h \quad (\text{eV}) \quad (5a)$$

and

$$H_m^I = 0.981 - 0.039 \times P_h \quad (\text{eV}), \quad (5b)$$

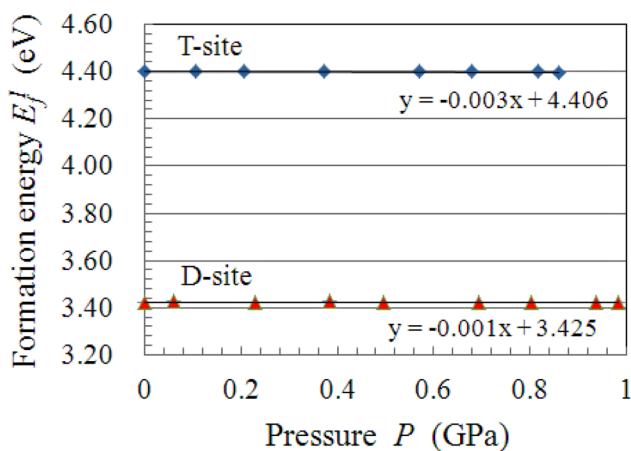


FIG. 3. Calculated dependence of formation energy E_f^I for D-site and T-site on the pressure P up to 1 GPa. Gap-correction and finite-size correction were performed to E_f^I for T-site.

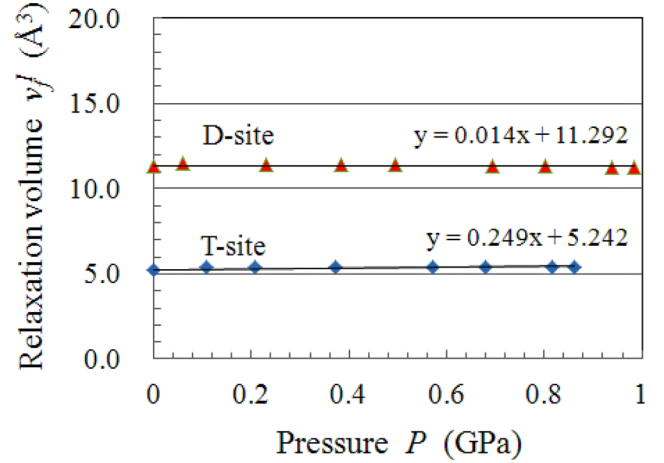


FIG. 4. Calculated dependence of relaxation volume v_f^I for D-site and T-site on the pressure P up to 1 GPa.

with P_h given in GPa. This result indicates that hydrostatic pressure leads to an increase of the equilibrium concentration and diffusion of self-interstitials.

B. Vacancies under hydrostatic pressure

For vacancies V , the neighboring atoms will tend to re-bond in ways that make the defect less symmetric, particularly in a covalently bonded crystal like Si. If the atoms are forced to maintain a T_d symmetry, the four neighbors draw in toward the center, pulling the rest of the lattice with them. However, the ground state involves a $T_d \rightarrow D_{2d}$ symmetry-breaking relaxation by Jahn–Teller distortion. For the neutral vacancy in Si, the Jahn–Teller distortion is now well-established by experiment³⁴ and theory.¹⁰ The four neighbors of the vacancy, labeled 1, 2, 3, and 4, move away from the sites they occupy in the perfect crystal forming two pairs (atom 1 with 2, and atom 3 with 4) as indicated by the arrows in Fig. 6. In the present study using GGA, the distance between the atoms in each pair of the un-relaxed vacancy is 3.864 Å at $P=0$. We found two type distortions with D_{2d} symmetry, which is similar to the results of Antonelli *et al.*¹³ In the first distortion labeled h -JT of the ground state, the distance between the atoms in each pair (atom 1 with 2, and atom 3 with 4) is 2.993 Å, and the distance between atoms belonging to different pairs is 3.508 Å at $P=0$. In the second distortion labeled l -JT, the distance between the atoms in each pair (atom 1 with 2, and atom 3 with 4) is 3.609 Å, and the distance between atoms belonging to different pairs is 3.428 Å at $P=0$.

TABLE I. DFT results for relaxation volume v_f^I and formation volume ($-\Omega_{Si} + v_f^I$) for self-interstitial at $P=0$.

Authors	Geometries of self-interstitials	Relaxation volume (Å ³)	Formation volume (Å ³)
Present work	D-site	11.292	-9.100
	T-site	5.242	-15.150
Centoni <i>et al.</i> ¹¹	D-site	13.84	-6.5
	T-site	7.54	-12.8

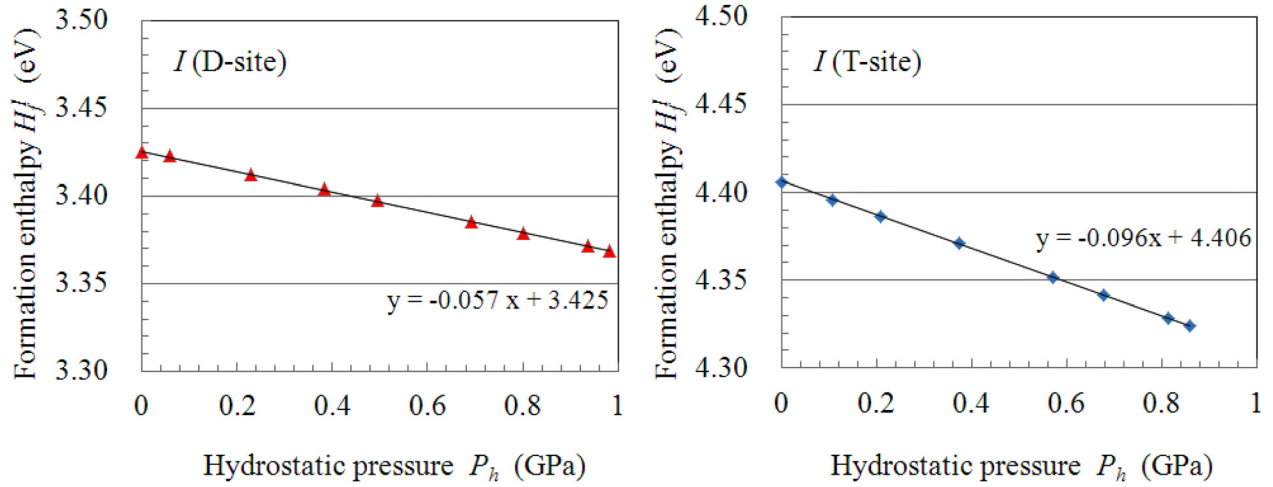


FIG. 5. Dependence of formation enthalpy H_f^I for D-site (left) and T-site (right) on the hydrostatic pressure P_h obtained with Eq. (3a).

Figure 7 shows the calculated dependence of the formation energy E_f^V for the vacancy with T_d symmetry, D_{2d} symmetry (h -JT and l -JT), and a so-called split-vacancy on the pressure P up to 1 GPa. The split- V has a configuration whereby one Si atom is at the bond center between two empty sites. This can be seen as a transition point for vacancy migration. It was found that E_f of V is almost constant under for pressures up to 1 GPa. The Jahn–Teller distortion of h -JT ($E_f = 3.543$ eV) reduces the formation energy by about 0.229 eV from T_d symmetry at $P = 0$. The distortion of l -JT gives slightly lower energy of about 0.024 eV compared to T_d symmetry at $P = 0$. The migration energy of V (h -JT is the ground state and split- V is the transition state) is 0.249 eV at $P = 0$. The obtained formation energy for the neutral V with Jahn–Teller distortion is in the range of previous DFT studies with GGA, which are most falling between 3.2 eV and 3.7 eV.¹⁰ The obtained $H_f^V + H_m^V (= 3.792$ eV) at $P = 0$ is considerably lower than the older experimental

value of 4.86 eV (Ref. 31) and the more recent value of 4.56 eV.^{32,33} Possible reasons for this significant difference between DFT calculations and experiment are not discussed further in the present paper as the main focus is to estimate the pressure effect on the formation and migration enthalpies.

Figure 8 shows the calculated dependence of the relaxation volume v_f^V for the vacancy on the pressure P up to 1 GPa. In contrast to I , the relaxation volumes v_f^V of V decrease linearly with increasing pressure P . It is interesting that the formation volume ($\Omega_{Si}(P) + v_f^V(P)$) becomes negative for h -JT and split- V for P between 0 and 1 GPa. For l -JT, the formation volume becomes negative when P is larger than 0.4 GPa. For T_d symmetry, discontinuous reduction of the relaxation volume was observed around $P = 0.2$ GPa. At this point, the distance between the atoms in each pair suddenly decreased. The relaxation volume, v_f^V , and the formation volume ($\Omega_{Si} + v_f^V$) of h -JT, l -JT, T_d symmetry, and split- V at $P = 0$ are summarized in Table II with the reported DFT results of negative formation volumes for V with Jahn–Teller distortion.^{11,13,35,36}

Figure 9 shows the dependence of the formation enthalpy H_f^V for h -JT (most stable) and split- V (transition state) on the hydrostatic pressure P_h obtained with Eq. (3b). It was found that the formation enthalpies of h -JT and split- V decrease with the square of the hydrostatic pressure P_h increase. The calculations lead to H_f^V and H_m^V dependencies on P_h given by

$$H_f^V = 3.543 - 0.021 \times P_h^2 - 0.019 \times P_h \quad (\text{eV}) \quad (6a)$$

and

$$H_m^V = 0.249 + 0.018 \times P_h^2 - 0.037 \times P_h \quad (\text{eV}), \quad (6b)$$

with P_h given in GPa.

These results indicate that hydrostatic pressure leads to a slight increase of the equilibrium concentration and diffusion of vacancies but this increase is, however, considerably smaller than that of self-interstitials. By the recombination between vacancies and self-interstitials, the hydrostatic pressure makes Si crystals more interstitial-rich. The results we

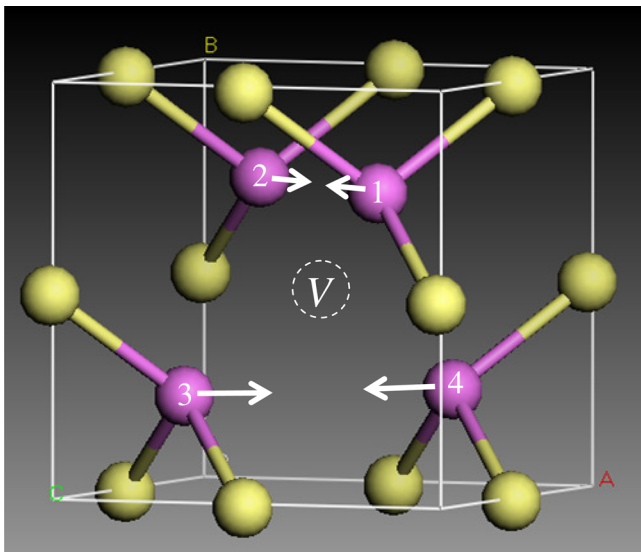


FIG. 6. Crystal structure of the un-relaxed vacancy in Si showing the atoms that are first (purple) and second (yellow) nearest neighbors of the vacancy. The arrows indicate the pairing of the first nearest neighbors by Jahn–Teller distortion.

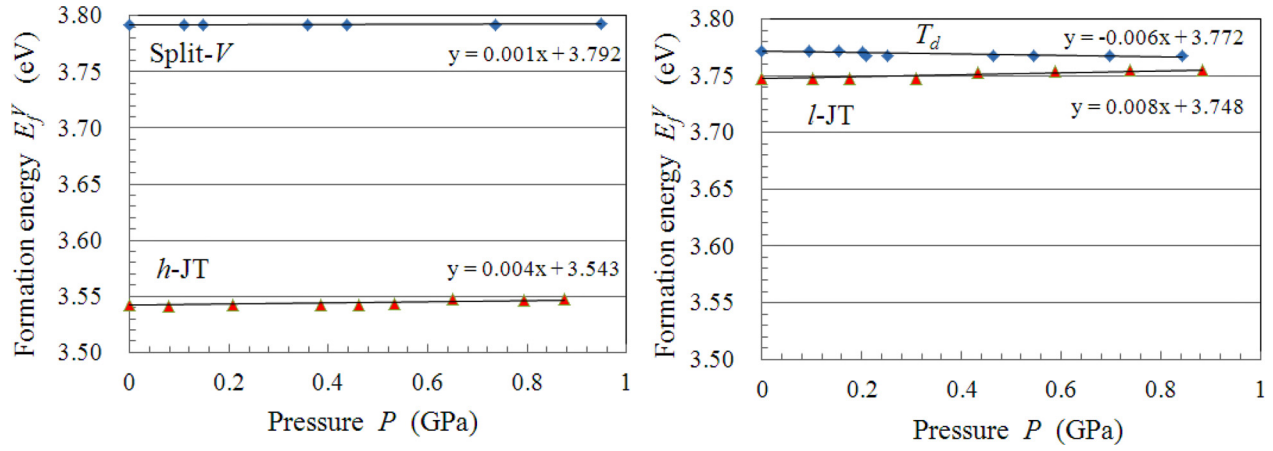


FIG. 7. Calculated dependence of formation energy E_f^V for vacancy with D_{2d} symmetry (h -JT) and split vacancy (left), and T_d symmetry and D_{2d} symmetry (l -JT) (right) on the pressure P up to 1 GPa.

obtained are consistent with the experimental results where hydrostatic pressure enhances the diffusivity of B through an interstitial-based mechanism³⁷ while it retards the diffusivity of Sb through a vacancy mechanism³⁸ in Si.

C. Self-interstitials and vacancies under internal pressure

Here, we move to the topic of thermal stress σ in Si during crystal growth. To simplify the explanation, the melt/solid interface and the peripheral surfaces are assumed to be free of external stresses. In this case, we can use Eqs. (4a) and (4b) to obtain the formation enthalpies of $H_f^I(P_{in})$ and $H_f^V(P_{in})$ under internal pressure P_{in} ($=\sigma$).

Figure 10 shows the changes in formation enthalpies ΔH_f^I for D- and T-sites, and ΔH_f^V for h -JT (most stable) and split- V (transition state) due to internal pressure P_{in} . We found that the H_f^I of I increases while the H_f^V of V decreases with the increase in P_{in} . The calculations lead to the dependencies of H_f^I , H_m^I and H_f^V , H_m^V on P_{in} given by

$$H_f^I = 3.425 + 0.070 \times P_{in} \quad (\text{eV}), \quad (7a)$$

$$H_m^I = 0.981 - 0.038 \times P_{in} \quad (\text{eV}), \quad (7b)$$

and

$$H_f^V = 3.543 - 0.160 \times P_{in} \quad (\text{eV}), \quad (7c)$$

$$H_m^V = 0.249 - 0.026 \times P_{in} \quad (\text{eV}), \quad (7d)$$

with P_{in} given in GPa.

These results indicate that compressive thermal stress leads to increases in the equilibrium concentration and diffusion of vacancies and to a decrease in the equilibrium concentration of self-interstitials. By the recombination between vacancies and self-interstitials, compressive thermal stress makes Si crystals more vacancy-rich.

It is noticeable that the impact of hydrostatic pressure and internal pressure on point defects is opposite. That is, hydrostatic pressure makes Si crystal more interstitial-rich, while internal pressure makes Si crystal more vacancy-rich. The main reason for this opposite impact is whether we include the contribution of $P\Omega_{Si}$ in the enthalpies or not, as mentioned in the Introduction.

Here, we briefly comment on the previous studies¹⁵ under biaxial compressive stress, in which the contribution of $P\Omega_{Si}$ should not be included as well as the case of thermal stress in growing single crystal Si. This is because Si samples under the biaxial mode have surfaces free of external stress. The experimental results revealed that biaxial stress retards the diffusivity of B through an interstitial-based mechanism

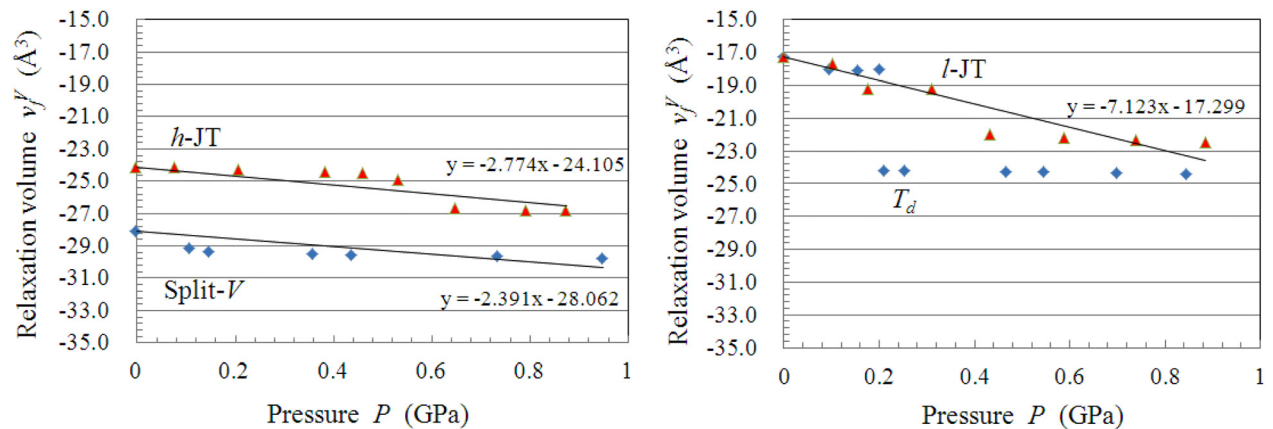


FIG. 8. Calculated dependence of relaxation volume v_f^V for vacancy with D_{2d} symmetry (h -JT) and split vacancy (left), and T_d symmetry and D_{2d} symmetry (l -JT) (right) on the pressure P up to 1 GPa.

TABLE II. DFT results for relaxation volume v_f^V and formation volume ($\Omega_{Si} + v_f^V$) for vacancy at $P = 0$.

Authors	Geometries of vacancies	Relaxation volume (\AA^3)	Formation volume (\AA^3)
Present work	<i>h</i> -JT	-24.105	-3.713
	<i>l</i> -JT	-17.299	3.093
	T_d symmetry	-17.299	3.093
	split- <i>V</i>	-28.062	-7.671
Centoni <i>et al.</i> ¹¹	Jahn-Teller distortion	-20.74	-0.4
Antonelli <i>et al.</i> ¹³	Jahn-Teller distortion	-21.4	-1.7
Sugino and Oshiyama ³⁵	Jahn-Teller distortion	...	-6.7
Windl <i>et al.</i> ³⁶	Jahn-Teller distortion	...	-2.0

while it enhances the diffusivity of Sb through a vacancy mechanism.¹⁵ These results are opposite to those under hydrostatic pressure¹⁵ described in the last part of Sec. III B, and the difference can be qualitatively explained whether the contribution of $P\Omega_{Si}$ to the enthalpies is taken into consideration or not.

D. Impact of thermal stress on $\Gamma 0_{\text{crit}}$

The “Voronkov criterion” $\Gamma 0_{\text{crit}}$ can be written as^{1,9}

$$\Gamma 0_{\text{crit}} \approx \frac{C_I^{eq}(T_m)D_I(T_m)E_f^I - C_V^{eq}(T_m)D_V(T_m)E_f^V}{[C_V(T_m) - C_I(T_m)]k(T_m)^2}. \quad (8)$$

C_I , C_I^{eq} and C_V , C_V^{eq} are the actual and the equilibrium self-interstitial and vacancy concentration, respectively. D_I and D_V are the self-interstitial and vacancy diffusivity, respectively. T_m is the melt temperature and k is the Boltzmann constant. E_f^I and E_f^V are the formation energy of the self-interstitial and vacancy, respectively.

In first order approximation, the impact of the thermal stress on $\Gamma 0_{\text{crit}}$ is obtained by replacing the formation and migration energies in Eq. (8) by the enthalpies obtained in this study and by using the thermal equilibrium concentrations at melt temperature, corresponding with these new formation enthalpies. To illustrate the impact of the thermal stress, the values of the formation and migration enthalpies as a function of internal pressure P_{in} given by Eqs. (7a)–(7d) were used. At $P_{in} = 0$, the thermal equilibrium concentrations

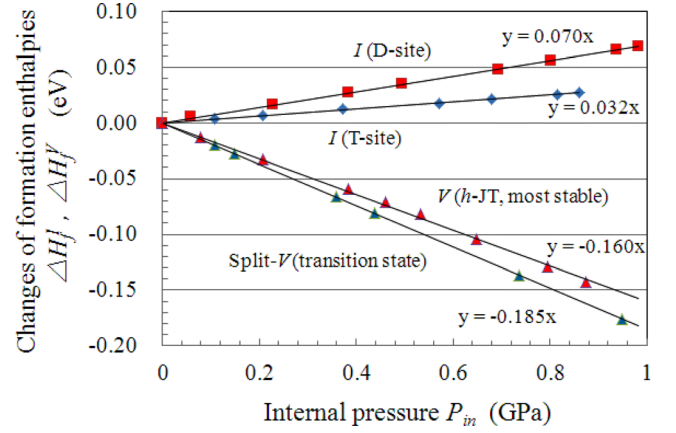


FIG. 10. Changes in formation enthalpies ΔH_f^I for D- and T-sites, ΔH_f^V for *h*-JT (most stable) and split-*V* (transition state) due to internal pressure P_{in} obtained with Eqs. (4a) and (4b).

and the diffusivities of point defects proposed by one of the authors are used⁹

$$C_I^{eq} = (2.276 \times 10^{27} \text{cm}^{-3}) \exp\left(\frac{-4.11 \text{eV}}{kT}\right), \quad (9a)$$

$$C_V^{eq} = (2.518 \times 10^{27} \text{cm}^{-3}) \exp\left(\frac{-4.11 \text{eV}}{kT}\right) \quad (9b)$$

and

$$D_I = (0.0655 \text{cm}^2 \text{s}^{-1}) \exp\left(\frac{-0.84 \text{eV}}{kT}\right), \quad (9c)$$

$$D_V = (0.000854 \text{cm}^2 \text{s}^{-1}) \exp\left(\frac{-0.45 \text{eV}}{kT}\right). \quad (9d)$$

Hereby, it is implicitly assumed that the pre-exponential factors of thermal equilibrium and diffusivity are not affected.

Figure 11 shows the dependence of $\Gamma 0_{\text{crit}}$ on compressive thermal stress $\sigma 0 = P_{in}$, where the results obtained by using the values for formation and migration enthalpies under hydrostatic pressure P_h in Eqs. (5) and (6) have also been given. A nearly linear relation between $\Gamma 0_{\text{crit}}$ (in $10^{-3} \text{cm}^2 \text{min}^{-1} \text{K}^{-1}$) and $\sigma 0$ (in MPa) is obtained, given by

$$\Gamma 0_{\text{crit}} \approx 1.509 - 0.023\sigma 0. \quad (10)$$

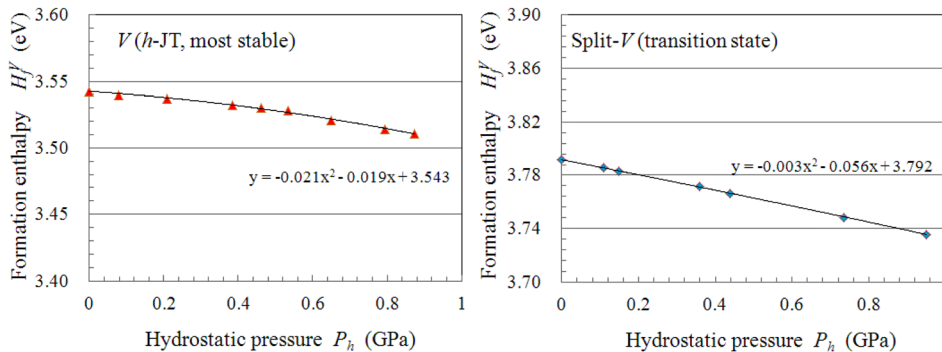


FIG. 9. Dependence of formation enthalpy H_f^V for *h*-JT (most stable) (left) and split-*V* (transition state) (right) on the hydrostatic pressure P_h obtained with Eq. (3b).

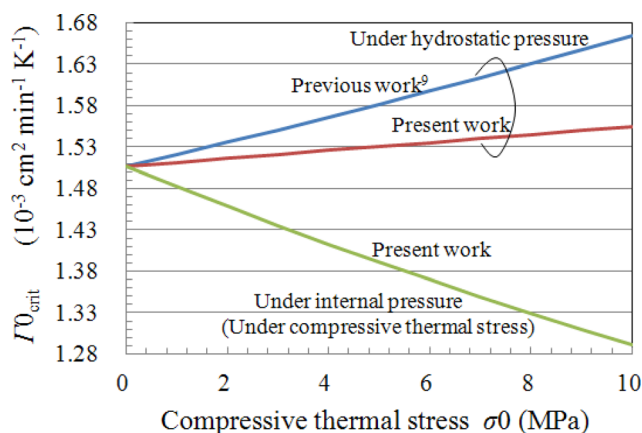


FIG. 11. Variations in critical v/G ratio Γ_{0crit} with compressive thermal stress $\sigma_0 = P_{in}$. Results obtained by using values for formation and migration enthalpies under hydrostatic pressure P_h are also given.

The impact of thermal stress on Γ_{0crit} is thus opposite to the estimates under hydrostatic pressure,⁹ and makes the growing Si crystal more vacancy-rich. The impact of stress affects the delicate intrinsic point defect balance in a narrow range to produce defect-free crystal. It is therefore important to take into account the impact of stress in Eq. (7a) in developing future large diameter defect-free crystals where average stress levels will probably be higher than those in smaller diameter crystals.

IV. CONCLUSIONS

The dependences of the formation enthalpy (H_f) and the migration enthalpy (H_m) of the self-interstitial I and the vacancy V on the hydrostatic pressure P_h and on the internal pressure P_{in} were calculated by calculating the formation energy (E_f) and relaxation volume (v_f). Density functional theory calculations were used with 216-atom supercells and with special attention for the convergence of the calculations.

The neutral I and V are found to have quasi constant formation energies E_f^I and E_f^V for pressures up to 1 GPa. For the relaxation volume, v_f^I is almost constant while v_f^V decreases linearly with increasing pressure P . The formation and migration enthalpies H_f^I and H_m^I , respectively, at the [110] dumbbell site are given by $H_f^I = 3.425 - 0.057 \times P_h$ (eV) and $H_m^I = 0.981 - 0.039 \times P_h$ (eV) with hydrostatic pressure P_h given in GPa. The H_f^V and H_m^V dependencies on hydrostatic pressure P_h are given by $H_f^V = 3.543 - 0.021 \times P_h^2 - 0.019 \times P_h$ (eV) and $H_m^V = 0.249 + 0.018 \times P_h^2 - 0.037 \times P_h$ (eV). These results indicate that hydrostatic pressure leads to a slight increase of the equilibrium concentration and diffusion of vacancies but this increase is considerably smaller than that of self-interstitials.

Next, the dependencies of formation enthalpies H_f^I for D- and T-sites, H_f^V for h -JT (most stable) and split- V (transition state) on internal pressure P_{in} were obtained. We found that the H_f^I of I increases while the H_f^V of V decreases with internal pressure P_{in} .

The results we obtained were used to more accurately describe the impact of thermal stress on Γ_{0crit} than the estimates under hydrostatic pressure. A nearly linear relation between Γ_{0crit} (in $10^{-3} \text{ cm}^2 \text{ min}^{-1} \text{ K}^{-1}$) and σ_0 (in MPa) was obtained, described by $\Gamma_{0crit} \approx 1.509 - 0.023\sigma_0$. The impact of thermal stress on Γ_{0crit} is thus opposite to the estimates under hydrostatic pressure and makes the growing Si crystal more vacancy-rich. The results illustrate that it is important to take into account the impact of stress on the generation of intrinsic point defects in developing future large diameter defect-free crystals.

ACKNOWLEDGMENTS

Jan Vanhellefont (Ghent University) is acknowledged for valuable discussion through this work. Kozo Nakamura (SUMCO Corporation) is acknowledged for the discussion on the formation volumes of point defects in perfect crystal Si.

- ¹V. V. Voronkov, *J. Cryst. Growth* **59**, 625 (1982).
- ²V. V. Voronkov and R. Falster, *J. Cryst. Growth* **194**, 76 (1998).
- ³W. von Ammon, E. Dornberger, H. Ölkug, and H. Weidner, *J. Cryst. Growth* **151**, 273 (1995).
- ⁴M. Hourai, E. Kajita, T. Nagashima, H. Fujiwara, S. Ueno, S. Sadamitsu, S. Miki, and T. Shigematsu, *Mater. Sci. Forum* **196–201**, 1713 (1995).
- ⁵E. Dornberger, D. Gräf, M. Suhren, U. Lambert, P. Wagner, F. Dupret, and W. von Ammon, *J. Cryst. Growth* **180**, 343 (1997).
- ⁶S. H. Lee, D. W. Song, H. J. Oh, and D. H. Kim, *Jpn. J. Appl. Phys., Part 1* **49**, 121303 (2010).
- ⁷E. Dornberger and W. von Ammon, *J. Electrochem. Soc.* **143**, 1648 (1996).
- ⁸T. Abe and T. Takahashi, *J. Cryst. Growth* **334**, 16 (2011) and references therein.
- ⁹J. Vanhellefont, *J. Appl. Phys.* **110**, 063519 (2011); *ibid.* **110**, 129903 (2011).
- ¹⁰B. Puchala, "Table 2.1 and 2.2," Ph.D. thesis, The University of Michigan, 2009 and references therein.
- ¹¹S. Centoni, B. Sadigh, G. Gilmer, T. Lenosky, T. Díaz de la Rubia, and C. Musgrave, *Phys. Rev. B* **72**, 195206 (2005).
- ¹²A. Antonelli and J. Bernholc, *Phys. Rev. B* **40**, 10643 (1989).
- ¹³A. Antonelli, E. Kaxiras, and D. Chadi, *Phys. Rev. B* **81**, 2088 (1998).
- ¹⁴M. Ganchenkova, A. Nazarov, and A. Kuznetsov, *Nucl. Instrum. Methods Phys. Res. B* **202**, 107 (2003).
- ¹⁵M. Aziz, *Mater. Sci. Semicond. Process.* **4**, 397 (2001) and references therein.
- ¹⁶The CASTEP code is available from Accelrys Software Inc.
- ¹⁷W. Kohn and L. Sham, *Phys. Rev.* **140**, A1133 (1965).
- ¹⁸D. Vanderbilt, *Phys. Rev. B* **41**, 7892 (1990).
- ¹⁹J. Perdew, K. Burke, and M. Ernzerhof, *Phys. Rev. Lett.* **77**, 3865 (1996).
- ²⁰G. Kresse and J. Furthmüller, *Phys. Rev. B* **54**, 11169 (1996).
- ²¹T. Fischer and J. Almlof, *J. Phys. Chem.* **96**, 9768 (1992).
- ²²M. Puska, S. Pöykkö, M. Pesola, and R. Nieminen, *Phys. Rev. B* **58**, 1318 (1998).
- ²³W. Windl, *ECS Trans.* **3**, 171–182 (2006).
- ²⁴H. Monkhorst and J. Pack, *Phys. Rev. B* **13**, 5188 (1976).
- ²⁵F. El-Mellouhi, N. Mousseau, and P. Ordejón, *Phys. Rev. B* **70**, 205202 (2004).
- ²⁶J. Poirier, *Introduction to the Physics of the Earth's Interior*, 2nd ed. (Cambridge University Press, New York, 2000).
- ²⁷O. Nielsen and R. Martin, *Phys. Rev. B* **32**, 3792 (1985).
- ²⁸T. Tsukada, M. Hozawa, and N. Imaishi, *J. Chem. Eng. Jpn.* **23**, 186 (1990).
- ²⁹W. Harrison, *Mater. Res. Soc. Symp. Proc.* **469**, 211 (1997).
- ³⁰B. Welber, C. Kim, M. Cardona, and S. Rodriguez, *Solid State Commun.* **17**, 1021 (1975).

- ³¹A. Ural, P. Griffin, and J. D. Plummer, [Phys. Rev. Lett.](#) **83**, 3454 (1999).
- ³²H. Bracht, [Phys. Rev. B](#) **75**, 035210 (2007).
- ³³H. Bracht, H. Silvestri, I. Sharp, and E. Haller, [Phys. Rev. B](#) **75**, 035211 (2007).
- ³⁴G. Watkins, [Mater. Res. Soc. Symp. Proc.](#) **469**, 139 (1997).
- ³⁵O. Sugino and A. Oshiyama, [Phys. Rev. B](#) **46**, 012335 (1992).
- ³⁶W. Windl, M. Daw, N. Carlson, and M. Laudon, [Mater. Res. Soc. Symp. Proc.](#) **677**, AA9.4.1 (2001).
- ³⁷Y. Zhao, M. Aziz, H. Gossmann, S. Mitha, and D. Schiferl, [Appl. Phys. Lett.](#) **74**, 31 (1999).
- ³⁸Y. Zhao, M. Aziz, H. Gossmann, S. Mitha, and D. Schiferl, [Appl. Phys. Lett.](#) **75**, 941 (1999).